JOURNAL OF MODERN OPTICS, 2000, VOL. 47, NO. 10, 1713–1728

Observation of sub-kilohertz resonance in Rf-Optical double resonance experiment in rare earth ions in solids

M. K. KIM‡, B. S. HAM*, P. R. HEMMER† and M. S. SHAHRIAR*

‡Dept. of Physics, University of South Florida, 4202 E. Fowler Avenue, Tampa, FL 33620 USA
*Research Laboratory of Electronics, Massachusetts Institute of Technology, Cambridge, MA 02139, USA
†Rome Laboratory, Hanscom Air Force Base, MA 01731, USA

(*Received 20 October 1999; revision received 8 March 2000*)

Abstract. We have observed kilohertz and sub-kilohertz resonance structures in RF-optical double resonance experiments of rare-earth-doped solids, when the frequency of the RF field is scanned across the hyperfine transitions while monitoring the resonant optical absorption of a CW laser. The effect is observed only when the laser spectral width is broad compared to the hyperfine structure. The observed line widths are apparently free of the inhomogeneous widths of hyperfine levels and the line shape has peculiar double peak structure. The effect is modelled with a resonance involving three atomic levels interacting with three electromagnetic fields, two optical and one RF, in a triangular or 'delta' configuration. While the ordinary optical-RF two-field resonance is limited by spin inhomogeneous width, the simultaneous excitation of three coupled transitions leads to narrow and highly nonlinear resonance structures that are not averaged by the inhomogeneous distribution of hyperfine transition.

1. Introduction

We have observed a peculiarly narrow resonance structure in the course of optical-RF double resonance experiment of rare earth ions in solids. The resonance is characterized by a sharp double peak structure in the absorption spectrum as the RF frequency is scanned across the hyperfine transition, with the few kilohertz width of the transparency hole at least an order of magnitude narrower than the spin inhomogeneous width. The effect is evident only when the laser bandwidth is larger than the hyperfine level splittings. A theoretical model is presented based on the assumption that the optical fields of a noisy laser simultaneously couples an optically excited state with two hyperfine levels of the ground state, which in turn are acted on by the RF field. A quantum interference effect among the three coupled transitions creates sharp fringes in the frequency domain that are not averaged out by ensemble average over the inhomogeneous broadening of the optical or spin transitions. The model is found to be consistent with the main features of the experimental observations.

Various quantum interference effects in atomic transitions have recently been research topics of great interest, because of the rich and often counter-intuitive

Journal of Modern Optics ISSN 0950–0340 print/ISSN 1362–3044 online
http://www.tandf.co.uk/journals

physics and their potential applications in nonlinear optical devices and spectroscopy. For example, in electromagnetically induced transparency (EIT) [1, 2], multiple paths of transitions created by the AC Stark effect of a strong coupling field can cause destructive interference and result in a transparency hole in the absorption spectrum. The effect is applied in enhanced harmonic generation [3, 4], wave mixing [5, 6], and amplification and laser action without population inversion [7–9]. Similar processes occur in coherent population trapping [10–13] of resonant Raman interaction [14, 15], where the spin coherence created by Raman optical fields gives rise to quantum interference and a transparency hole in the absorption spectrum. The spin coherence can be created by directly applying an RF field on the spin transition, and this also results in transparency [16]. In most of these systems, the basic process is an interaction of a three-level system with two electromagnetic fields, where the two transitions or some linear combinations interfere with each other to create a characteristic transparency hole in the absorption spectrum. A general requirement for observation of the transparency hole is that the coupling field be strong enough to overcome inhomogeneous broadening. For example, in resonant Raman interference, the optical Raman Rabi frequency needs to be large compared to the hyperfine inhomogeneous width [15] in order for coherent population trapping to produce an observable hole in the absorption spectrum. A few authors have investigated the interaction of closed loop transitions including a triangular resonance [17, 18], but it appears these studies have been restricted to cases of time-dependence and phase-dependence of the system response at exact resonance only.

There are a number of spectral line-narrowing processes that have made great contributions in the various areas of laser spectroscopy. Examples are laser induced fluorescence [19], spectral hole burning [20], Doppler-free spectroscopy by multiphoton processes [21], Ramsey resonance by separated fields [22], and various double resonance methods [23, 24]. Most often the strategy is to reduce or eliminate the effect of inhomogeneous broadening of the spectral lines, in order to reveal the natural or homogeneous line widths. The experiment described here started out as an optical-RF double resonance experiment, where the spectral line width is expected to be limited by the spin inhomogeneous width. The observed narrow resonance structure and the proposed theoretical model of three-level three-field interaction allows spectral resolution even below the spin inhomogeneous line width.

2. Experiment

The experiments are performed using the apparatus shown in figure 1, with a ring dye laser that provides about 500 mW of output. An acousto-optic modulator is used to turn the laser pulses on and off. The laser light then enters the sample crystal in a liquid helium cryostat. A 15-turn RF coil is wound around the crystal and the transmitted light through the crystal is detected by a photodiode. The RF field, up to 30 MHz, for the coil is generated using a synthesized function generator, which is switched and amplified up to 2 W power. A digital delay generator provides the timing signals. The detected signal is fed into a lock-in amplifier or to a digital oscilloscope, and a desktop computer running LabView controls all the digital instruments, and collects and processes the data. Data presented below utilize three different detection methods. One is lock-in amplifier

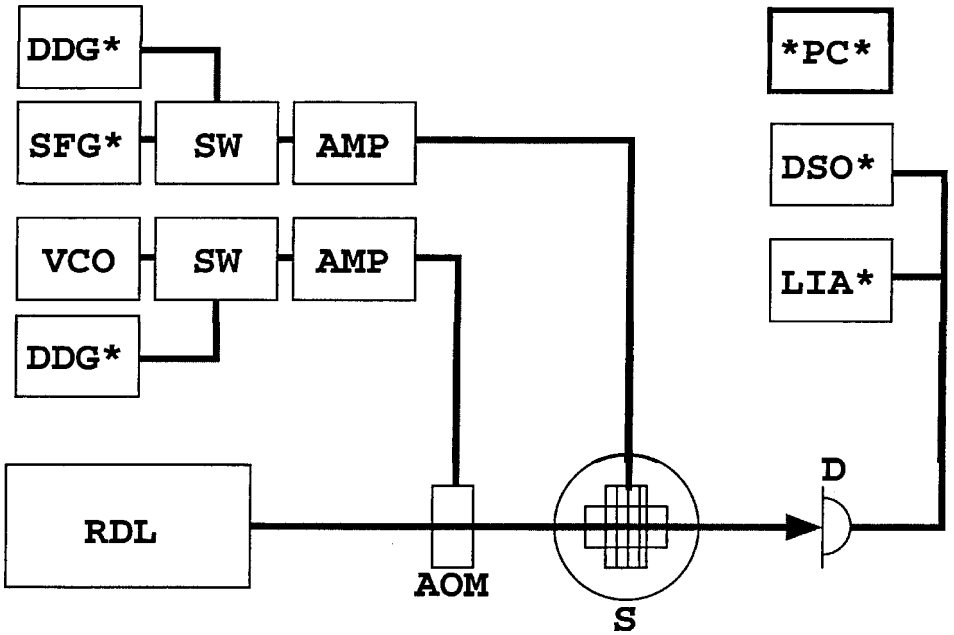

Figure 1. Schematic of apparatus. RDL: ring dye laser; AOM: acousto-optic modulator; S: sample crystal with RF coil inside a liquid helium cryostat; D: photodiode; DDG: digital delay generator; SFG: synthesized function generator; VCO: voltage controlled oscillator; SW: RF switch; AMP: 2W RF amplifier; DSO: digial oscilloscope; LIA: lock in amplifier; PC: desktop computer controlling digital devices (*).

output of transmitted optical signal with pulsed optical field and CW RF field ('optical lock-in signal'); another is lock-in amplifier output with CW optical field and pulsed RF field ('RF lock-in signal'); and the third is the output of digital oscilloscope showing averaged time signal of photodiode ('time signal').

Figure 2(*a*) shows an example of the observed resonance structure when the transmitted light is lock-in detected while the RF frequency is scanned near the 7 MHz hyperfine transition of the $^3H_4$ ground state. The sample is 0.1 at %Pr^{3+} : $YAlO_3$ of 17 mm length at temperature of 4.2 K. (See [23, 25–28] for spectroscopic details of Pr^{3+} : $YAlO_3$.) The optical field is tuned to the 610.53 nm $^3H_4 - ^1D_2$ transition, where the optical density of the crystal is ~ 0.4, or 30% absorption. For most of the measurements the optical field is chopped by the AOM at 1 kHz with 50% duty cycle, while the RF field is CW. Note the very narrow 2.1 kHz transparency hole centred at 7.1162 MHz. The vertical scale is proportional to the transmitted light and the figure indicates close to 70% maximum absorption, relative to off-resonance background, on either side of the central hole, but almost complete transmission at the centre of the hole. This was consistent with naked eye observation of the laser beam transmitted through the crystal. The structure disappears, however, when the laser frequency is stabilized to less than a few megahertz, as shown in Fig. 2(*b*), where the overall transmittance is higher (compared to figure 2(*a*)) because of spectral hole burning. (Even when the laser frequency is slowly scanned to reduce the spectral hole burning effect, the above resonance structure is not observed.) The ground state hyperfine transitions

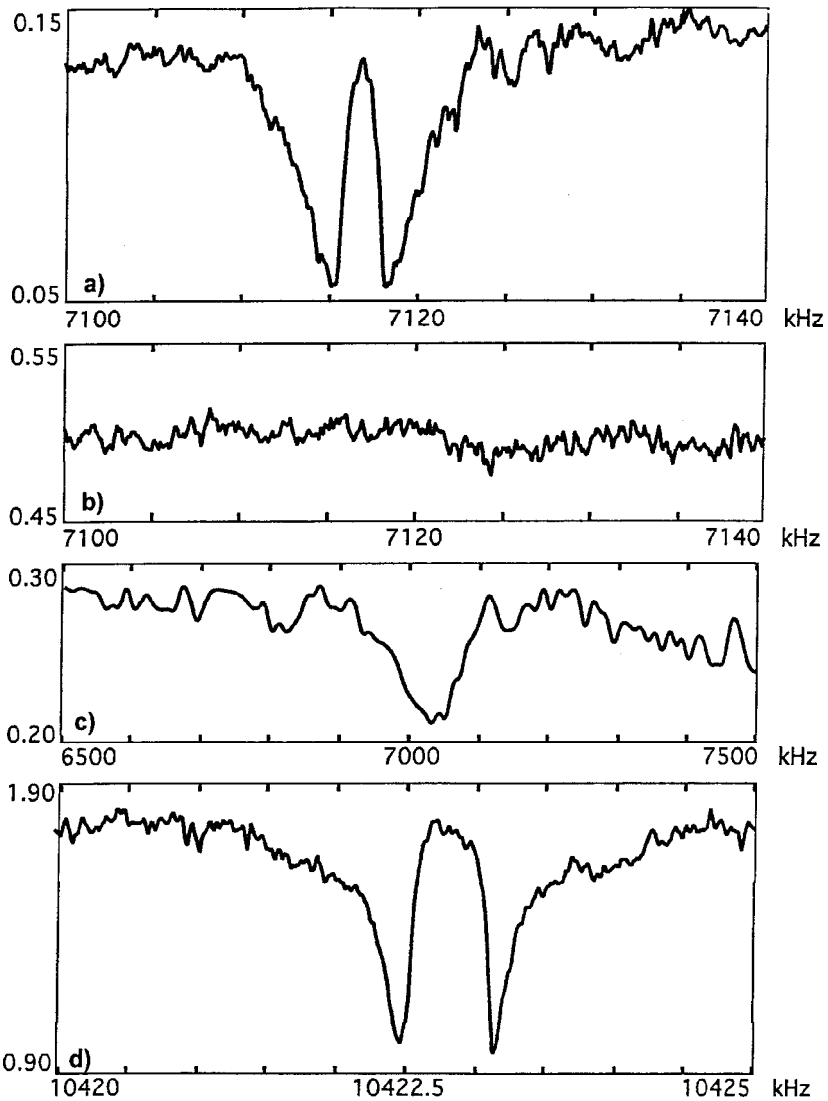

Figure 2. (*a*) Optical lock-in signal, in arbitrary units, versus RF frequency for $^3H_4$ to $^1D_2$ transition in $Pr^{3+}:YAlO_3$ near 7 MHz when the laser is not stabilized, and (*b*) when the laser is stabilized. For optical lock-in signal the optical field is pulsed at 1 kHz rate with 50% duty cycle while the RF field is cw. (*c*) The stimulated photon echo signal versus frequency of RF pulse applied during the 100 μs period between the second and third pulses of stimulated photon echo experiment. (*d*) Optical lock-in signal versus RF frequency for $^3H_4$ to $^1D_2$ transition in $Pr^{3+}:Y_2SiO_5$ near 10 MHz.

are known to have centre frequencies 7.057, 14.13, and 21.19 MHz with inhomogeneous widths of ~ 50 kHz. For comparison, figure 2(c) shows the hyperfine inhomogeneous line at 7.06 MHz transition as detected by photon echo nuclear double resonance (PENDOR). We have also found similar structures near the others of frequencies 14.233 MHz and 21.349 MHz, with the respective gap widths of 3.0 and 3.5 kHz. Furthermore, we have observed a 0.65 kHz gap structure at

10.433 MHz, figure 2(*d*), and 1.0 kHz gap structure at 17.390 MHz in $Pr^{3+}:Y_2SiO_5$, where the corresponding known hyperfine frequencies are 10.19 and 17.30 MHz with inhomogeneous width of ~ 40 kHz [29, 30]. As indicated above, a very important observational peculiarity is that these narrow transparency hole structures appear only when the laser is known to have large bandwidth compared to the hyperfine transition frequencies. When the laser stabilization circuit is locked to reduce the bandwidth to a few megahertz or less, the kilohertz hole structures disappear. The laser frequency structure is monitored with a Fabry–Perot interferometer to have about 40 MHz bandwidth when the stabilization was inactive, with additional fluctuation over ~ 100 MHz range. When the stabilization is locked the laser bandwidth is measured to be at most $3 \sim 4$ MHz, and had occasional mode-hops. The laser cavity mode spacing is 240 MHz.

We have studied experimentally the behaviour of the resonance structure with respect to a number of experimental parameters. For example, figure 3 shows that increasing the RF field strength broadens the width of the side wings proportionately, but the width of the gap remains constant. The RF circuit is not resonant or matched but if we assume a few gauss of RF magnetic field strength and 2.4 kHz/G gyromagnetic ratio of the $^3H_4$ hyperfine levels, the spin Rabi frequency is expected to be a few kilohertz. Figure 4 shows the behaviour when the optical field strength is varied using neutral density filters. There is a moderate but clear increase of the gap width as the optical power increases. The optical power that enters the sample is about 10 mW and the 2 mm diameter beam is focused by a 30 cm lens. If we assume a ratio (atomic homogeneous width)/(laser spectral width) $= 10^{-4}$ and oscillator strength of 3×10^{-7}, the optical Rabi frequency is

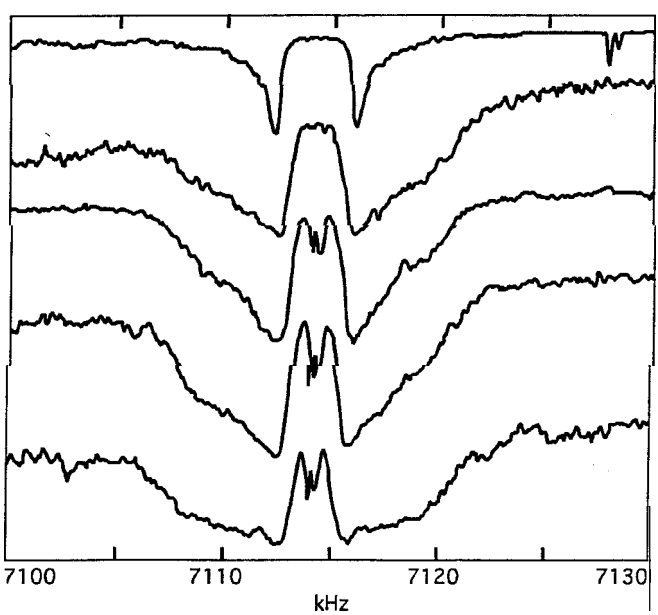

Figure 3. Optical lock-in signal versus RF frequency for varying RF field strengths. Relative RF field amplitudes, from top to bottom, is nominally 1:2:4:8:16. (Different lock-in amplifier gains have been used between different traces, so that the relative vertical scales should not be compared between them. The glitch on the right end of top trace is an experimental artefact.)

~ 3 kHz. Figure 5 shows the evolution of resonance lineshape as the pulse length is increased. The RF lock-in signal has zero background and the resonance curve displays distinct and reproducible structures. The RF pulse length is varied from 100 μs to 800 μs while the repetition rate is kept at 1 kHz. One can see the

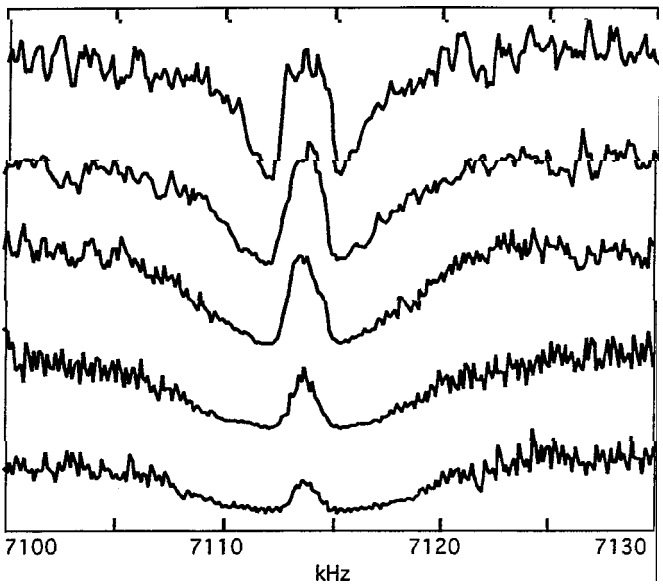

Figure 4. Optical lock-in signal versus RF frequency for varying optical field strengths. Neutral density filters of optical density, from top to bottom, 0.04, 0.5, 1.0, 1.5, and 2.0 are inserted before the sample. Another set of neutral density filters are used in front of the detector to adjust detectable signal levels.

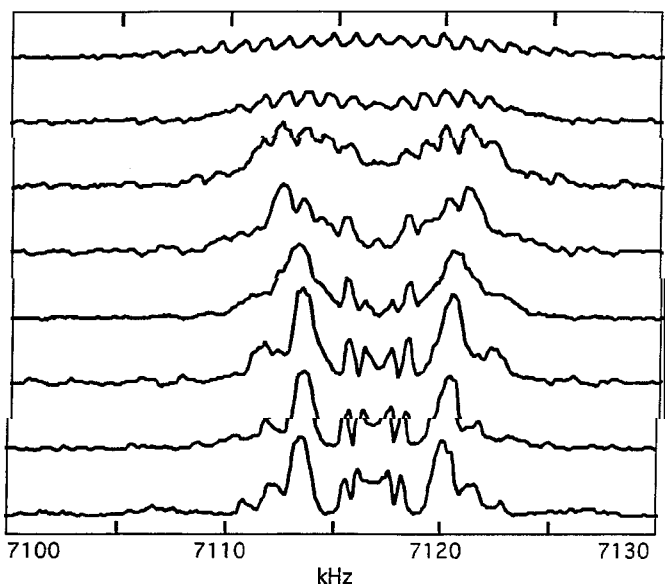

Figure 5. RF lock-in signal versus RF frequency for varying RF pulse length. For RF lock-in signal the optical field is CW while the RF field is pulsed at 1 kHz. The RF pulse lengths are, from top to bottom, 100, 200, 300, 400, 500, 600, 700, and 800 μs.

establishment of the resonance structure in a few hundred microseconds. Notice also the high degree of symmetry of the detailed lineshape with respect to the centre of the resonance. The high 'frequency' wiggle is due to the 1 kHz lock-in cycle. In order to ascertain that the main features of these observations are not artefacts of lock-in detection, we have acquired a 2.0-ms-long time signal, averaged 300 shots at 100 Hz repetition rate, of the transmitted light using a digital oscillosope, then scanned the RF frequency from 7.11 to 7.13 MHz in 0.5 kHz steps, to compose a time–frequency profile of the resonance structure. A result is shown in figure 6(*a*), where basically all the features of the frequency-domain data are reproduced, including the gradual sharpening of the double peak structure as a function of time. Figure 7 shows a few individual time signal traces for various RF frequencies. The observed resonance structure disappears quite abruptly when the temperature rises beyond 10 K; we have looked for similar effects in $Pr^{3+} : LaF_3$

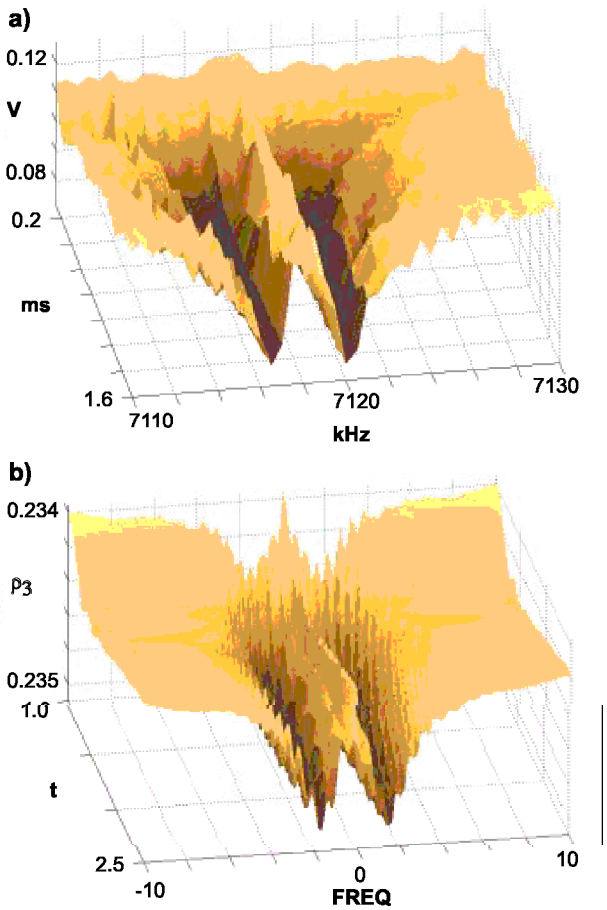

Figure 6. (*a*) Experimental and (*b*) calculated profiles of optical signals versus time and RF frequency. The vertical scale in (*a*) is the photodiode voltage measured on the oscilloscope, and in (*b*) it is the population of level $|3\rangle$, which is inverted in order to represent higher absorption with larger $|3\rangle$ state population. The parameters used in (*b*) are: $\Gamma_1 = \Gamma_2 = 1, \Gamma' = 0; \gamma_1 = \gamma_2 = 2\pi; \gamma' = 0.4\pi; \Omega_1 = \Omega_2 = 4\pi; \Omega' = 0.2\pi$; integrated over optical inhomogeneous width of 20, in steps of 0.5 and spin inhomogeneous width of 10, in steps of 0.5. The FREQ axis is $\Delta'/2\pi$.

but found none. We have also measured the resonance structure against RF frequency at various optical detuning, and only observed variations in overall signal size and some detailed shapes of the central peaks.

3. Theory

We propose to model the observed resonance effect as a three-level atomic system interacting with three electromagnetic fields (3L3F) in a delta-shape configuration, as shown in figure 8. The system consists of two hyperfine levels $|1\rangle$ and $|2\rangle$ of the ground state, with eigen energies ε_i ($i = 1,2$), and an optically

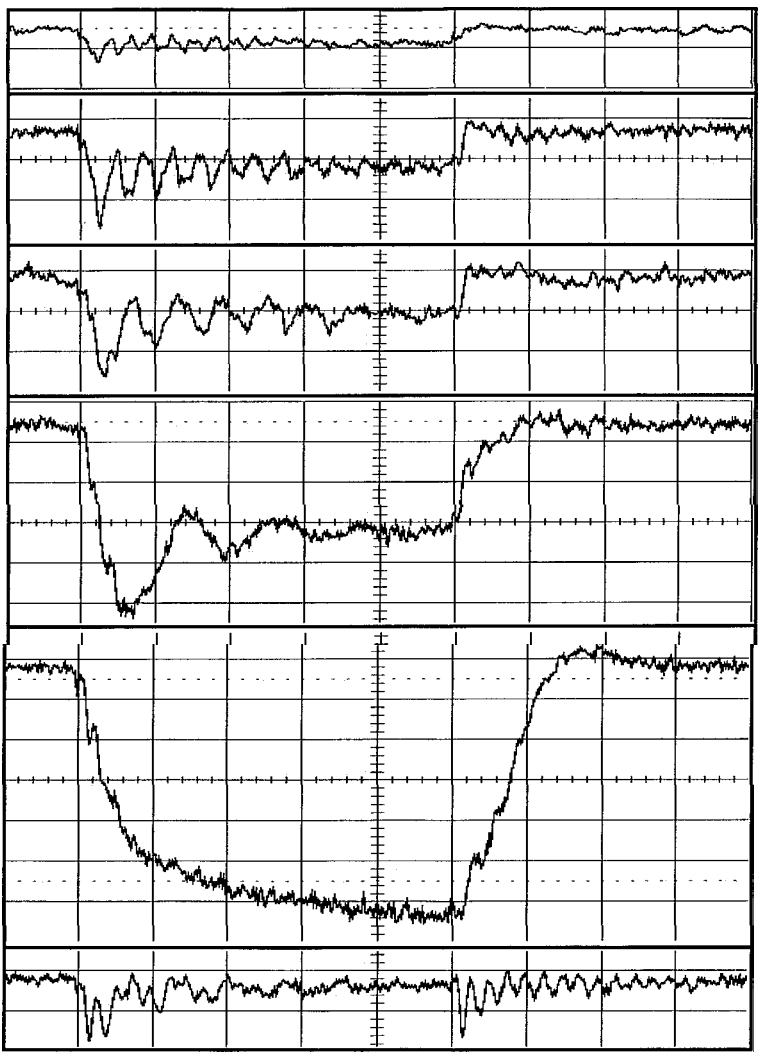

Figure 7. Oscilloscope time signal of transmitted light when 5-ms-long RF pulse is applied. The RF frequencies are, from top to bottom, 7110, 7111, 7112, 7113, 7114, and 7115 kHz. The horizontal scale is 1 ms/div and the signals are averaged for 1000 sweeps.

excited level $|3\rangle$, with $\varepsilon_3 = 0$. The optical field is $E = \frac{1}{2}\{E_1 e^{-i\omega_1 t} + E_2 e^{-i\omega_2 t}\} + \text{c.c.}$ and we assume that the E_i's couple the $|i\rangle - |3\rangle$ transitions independently, with Rabi frequencies $\Omega_i = (p_i E_i/2\hbar)(p_i : |i\rangle - |3\rangle$ transition electric dipole moments) and detuning parameters $\Delta_i = (\varepsilon_3 - \varepsilon_i)/\hbar - \omega_i$. (Note that the definition of Rabi frequency here is one half of the more conventional definition.) These transitions have population relaxation rates Γ_i, and phase relaxation rates γ_i. The two ground states $|1\rangle - |2\rangle$ are coupled by the RF magnetic field, with similarly defined parameters: field frequency, ω'; Rabi frequency of magnetic dipole transition, Ω'; detuning, $\Delta' = (\varepsilon_2 - \varepsilon_1)/\hbar - \omega'$; population relaxation rate, Γ'; and phase relaxation rate γ'.

The density matrix equation of motion [31, 32]

$$\frac{d}{dt}\rho_\omega = -\frac{i}{\hbar}[\mathscr{H}_\omega, \rho_\omega] + (\textit{relaxation terms}) \tag{1}$$

is written in a rotating reference frame defined with

$$U_\omega = \begin{bmatrix} e^{-i\omega_1 t} & 0 & 0 \\ 0 & e^{i\omega_2 t} & 0 \\ 0 & 0 & 1 \end{bmatrix} \tag{2}$$

so that

$$\rho_\omega = U_\omega \rho U_\omega^{-1} \equiv \begin{bmatrix} \rho_1 & \sigma' & \sigma_1 \\ \sigma'* & \rho_2 & \sigma_2 \\ \sigma_1^* & \sigma_2^* & \rho_3 \end{bmatrix}, \tag{3}$$

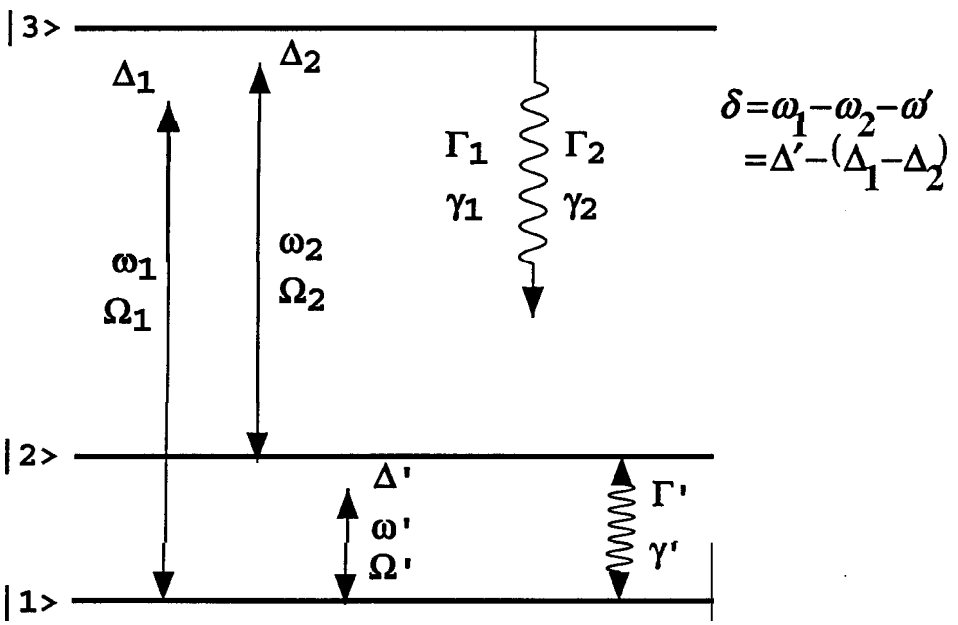

Figure 8. A three-level three-field (3L3F) system.

where $\rho = |\Psi\rangle\langle\Psi|$ is the density matrix in the lab frame. The Hamiltonian in this rotating frame is, with the three-photon resonance detuning $\delta = \Delta' - (\Delta_1 - \Delta_2)$,

$$\mathscr{H}_\omega = U_\omega \mathscr{H} U_\omega^{-1} + i\hbar\left(\frac{\mathrm{d}}{\mathrm{d}t}U_\omega\right)U_\omega^{-1} = \begin{bmatrix} -\hbar\Delta_1 & -\hbar\Omega' e^{-i\delta t} & -\hbar\Omega_1 \\ -\hbar\Omega' e^{i\delta t} & -\hbar\Delta_2 & -\hbar\Omega_2 \\ -\hbar\Omega_1 & -\hbar\Omega_2 & 0 \end{bmatrix}, \quad (4)$$

The rotating wave approximation is used where we neglect the terms of frequencies $2\omega_1$ and $2\omega_2$ compared to DC terms, as well as the terms of frequency $(\omega_1 - \omega_2 + \omega')$ compared to $\delta = (\omega_1 - \omega_2 - \omega')$. Notice that this Hamiltonian is time dependent. For a three-level three-field system, it is in general not possible to find a rotating frame that completely removes the time-dependence of the Hamiltonian. The explicit form of the equations of motion (1) is written out as:

$$\begin{aligned}
\dot{\rho}_1 &= -i\Omega_1(\sigma_1 - \sigma_1^*) - i\Omega'(e^{+i\delta t}\sigma' - e^{-i\delta t}\sigma'^*) + \Gamma_1\rho_3 - \tfrac{1}{2}\Gamma'(\rho_1 - \rho_2) \\
\dot{\rho}_2 &= -i\Omega_2(\sigma_2 - \sigma_2^*) + i\Omega'(e^{+i\delta t}\sigma' - e^{-i\delta t}\sigma'^*) + \Gamma_2\rho_3 + \tfrac{1}{2}\Gamma'(\rho_1 - \rho_2) \\
\dot{\rho}_3 &= +i\Omega_1(\sigma_1 - \sigma_1^*) + i\Omega_2(\sigma_2 - \sigma_2^*) - (\Gamma_1 + \Gamma_2)\rho_3 \\
\dot{\sigma}_1 &= -i\Omega_1(\rho_1 - \rho_3) + i\Omega' e^{-i\delta t}\sigma_2 - i\Omega_2\sigma' - (\gamma_1 - i\Delta_1)\sigma_1 \\
\dot{\sigma}_2 &= -i\Omega_2(\rho_2 - \rho_3) + i\Omega' e^{+i\delta t}\sigma_1 - i\Omega_1\sigma'^* - (\gamma_2 - i\Delta_2)\sigma_2 \\
\dot{\sigma}' &= -i\Omega' e^{-i\delta t}(\rho_1 - \rho_2) - i\Omega_2\sigma_1 + i\Omega_1\sigma_2^* - (\gamma' - i(\Delta_1 - \Delta_2))\sigma'.
\end{aligned} \quad (5)$$

Because of the time dependence, it is not possible to write a formal solution to the density matrix equation using matrix exponential, and it appears rather difficult to discern the general behaviour of the solution. However, an analogy with a single-function equation of motion, in the form $\mathrm{d}z/\mathrm{d}t = [-\gamma + i\Omega + i\Omega' e^{i\delta t}]z(t)$ may be made whose solution contains a factor for example $z \sim \cos[\sin \delta t/(\delta/\Omega')]$. Because of the sinc function argument in the cosine, there are rapid oscillations as δ approaches zero. Numerical calculation of the three-level system displays analogous behaviour, as will be seen below. This rapid oscillation washes out any inhomogeneous distribution of the detuning parameter δ, except at the exact centre of the distribution.

The equation of motion (equation (5)) is solved numerically using a Runge–Kutta method on MatLab. Single-atom solutions are then accumulated over the inhomogeneous distribution of the spin and optical transitions. The level $|3\rangle$ population ρ_3 is plotted as a measure of optical absorption, as a function of RF detuning Δ'. The top trace of figure 9(*a*) shows a result of such calculation. The separation of the double peak is the Raman Rabi frequency $2\Omega = 2\sqrt{\Omega_1^2 + \Omega_2^2}$. On top of the double peak structure, there is a rapid oscillation in frequency domain with period of $1/2t$. The width of each of the double peaks is proportional to the spin Rabi frequency, but the optical dephasing γ also broadens it. Also note that the centre of the resonance is exactly zero with respect to the off-resonance background. (For the top trace of figure 9(*a*) the off-resonance background level is $\rho_3 = 0.217$ and the peak level is 0.226, so that the peak represents $< 50\%$ change in calculated ρ_3.) This 3L3F solution is contrasted with a three-level two-field (3L2F) solution in figure 9(*b*), where there are one optical and one RF fields, corresponding to a normal optical-RF double resonance experiment. Again the double peak separation corresponds to optical Rabi frequency for AC Stark effect.

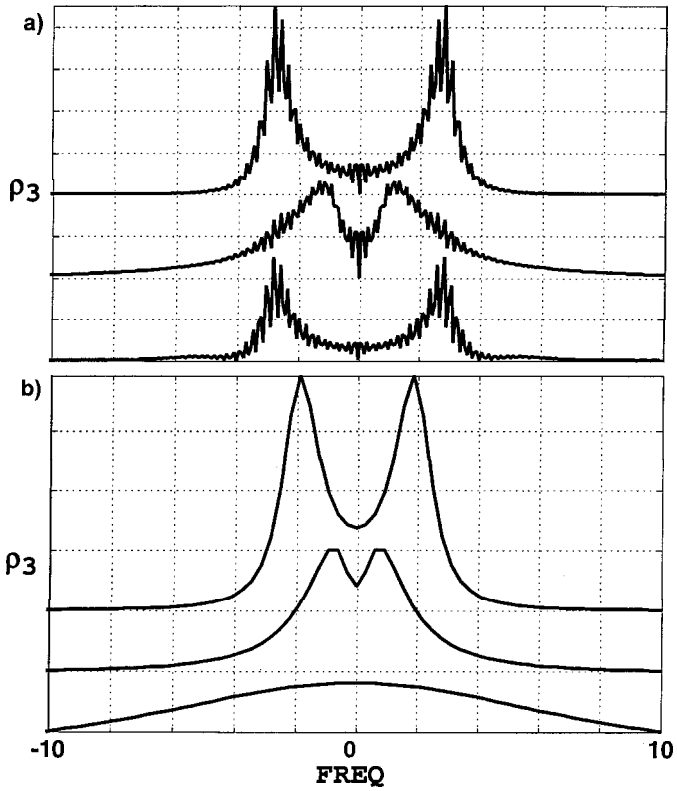

Figure 9. (a) Calculated profile of 3L3F resonance, ρ_3 vs. $\Delta'/2\pi$. Top: Single atom calculation: $\Gamma_1 = \Gamma_2 = 1$; $\Gamma' = 0$;$\gamma_1 = \gamma_2 = 2\pi$; $\gamma' = 0.4\pi$; $\Omega_1 = \Omega_2 = 4\pi$; $\Omega' = 0.2\pi$; $\Delta_1 = \Delta_2 = 0$; $t = 2.5$. Middle: Integrate over optical inhomogeneous width of 20, in steps of 0.4. Bottom: Integrate over spin inhomogeneous width of 20, in steps of 0.4. (*b*) Calculated profile of 3L2F resonance. All parameters are the same as in (*a*), except that $\Omega_2 = 0$.

Note that there is no rapid oscillation structure, and that the resonance centre is above zero with respect to the off-resonance background. There appear marked differences between the two-field and three-field solutions when they are integrated over the inhomogeneous broadening of atoms. For the 3L2F case, the double peak stucture is smeared out immediately when it is integrated over the spin inhomogeneous width and the integrated resonance curve has the spin inhomogeneous width. On the other hand, there is no qualitative change in the resonance shape of the 3L3F solution when it is integrated over the spin inhomogeneous width. When integrated over the optical broadening, the gap between the double peak narrows but remains non-zero. One also notices that there is a qualitative change in the resonance line shape and that the centre of resonance is still zero with respect to the off-resonance background.

Next let us examine the behaviour of the 3L3F solution, integrated over optical inhomogeneous width, with respect to various parameters. Figure 10 shows its dependence on the spin Rabi frequencies. As the spin Rabi frequency increases, the width of the wings increase proportionately and the amplitude of the signal

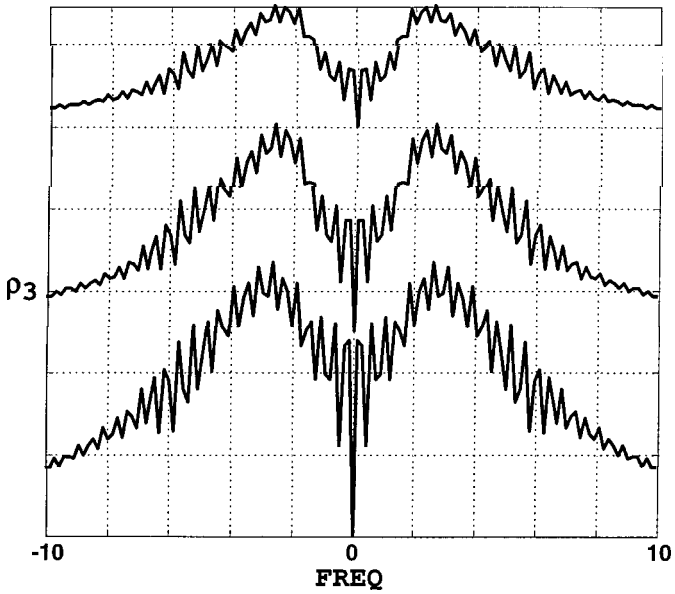

Figure 10. Calculated profile of 3L3F resonance for varying spin Rabi frequencies: from top to bottom, $\Omega' = 0.2\pi$, 0.4π, 0.8π. All other parameters are the same as in the middle trace of figure 9(*a*).

increases as the square of the Rabi frequency, but the width of the gap does not change. The increase of optical Rabi frequency results (figure 11) in the proportionate increase of the gap width. On the other hand, the numerical experiments show that the gap width and structure are also dependent on the phase relaxation rates of the spin and optical transitions. In figure 12, the increase in spin phase relaxation rate γ' results in reduction of the overall resonance structure but the resonance widths remain the same. Quite unexpectedly however, when the optical phase relaxation rate γ is increased in figure 13, the resonance structure becomes narrower and sharper. The population relaxation rates Γ do not affect the resonance shape appreciably. Figure 6(*b*) shows the time–frequency plot of the resonance for a particular set of parameters indicated in the caption.

4. Discussion

The numerical analysis based on the model of three-level atoms interacting with three electromagnetic fields has several important features that are consistent with the experimental observations. First, the resonance lineshape has the distinct double-peak structure. The width of the gap is very small compared to the inhomogeneous width of the spin transition. This double peak structure is averaged out and absent in the case of two-field RF-optical double resonance. Also notice that the shape of the calculated resonance structure, integrated over optical linewidth, has the distinct shape observed experimentally. Second, there is the fringe pattern in the frequency domain with 'period' equal to the inverse of the pulse length. Third, the increase of the width of the wings with respect to the RF

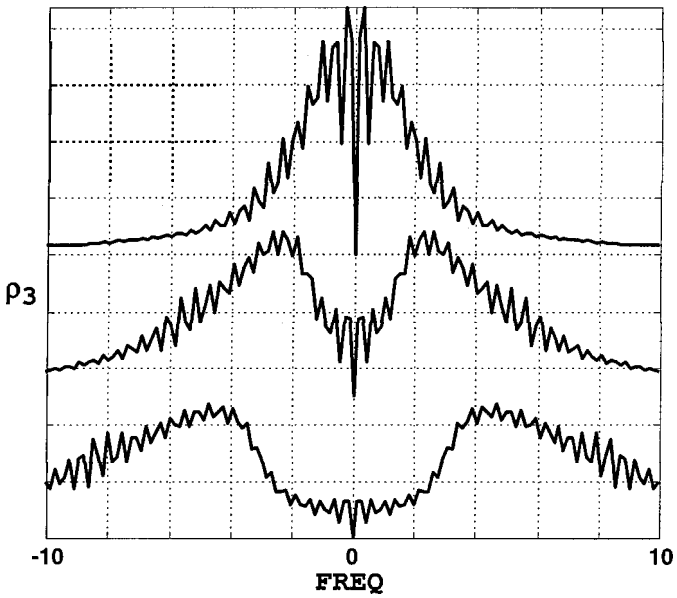

Figure 11. Calculated profile of 3L3F resonance for varying optical Rabi frequencies: from top to bottom, $\Omega_1 = \Omega_2 = 2\pi, 4\pi, 6\pi$. All other parameters are the same as in the middle trace of figure 9(*a*).

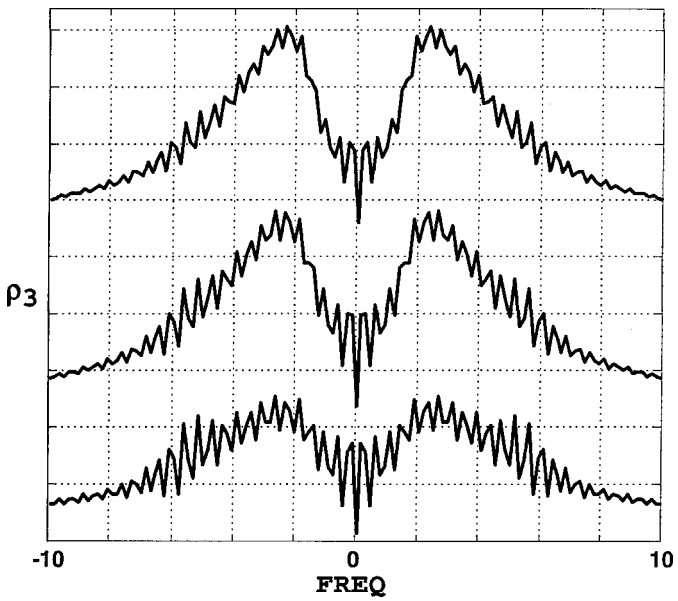

Figure 12. Calculated profile of 3L3F resonance for varying spin phase relaxation rates: from top to bottom, $\gamma' = 0.2\pi, 0.4\pi, 0.8\pi$. All other parameters are the same as in the middle trace of figure 9(*a*).

field strength is well verified by the experiment. With an estimated few gauss of RF magnetic field strength and 2.4 kHz/G gyromagnetic ratio of the $^3H_4$ hyperfine levels, the spin Rabi frequency is expected to be a few kilohertz. Although the

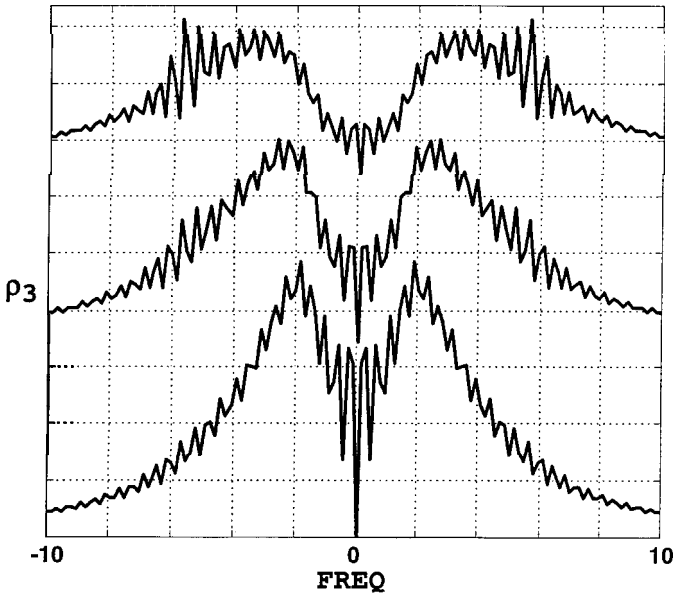

Figure 13. Calculated profile of 3L3F resonance for varying optical phase relaxation rates: from top to bottom, $\gamma_1 = \gamma_2 = 1\pi, 2\pi, 4\pi$. All other parameters are the same as in the middle trace of figure 9(*a*).

magnetic field is not calibrated, at least the order of magnitude appears reasonable. But more importantly, the wing width does increase in proportion with the field strength. As for the dependence of the gap width on the optical Rabi frequency, the experimental data shows much slower than the linear dependence seen in the theory. One may attribute this tentatively to the effect of the optical phase relaxation. The gap width calculated according to the theoretical model appears to be determined by the optical Rabi frequency, but the optical phase relaxation also narrows the gap width. This behaviour is very nonlinear and it is difficult to predict the gap width in terms of experimental parameters, except to say that the maximum gap width is proportional to the optical Rabi frequency. Some of the numerical results suggest that the optical phase relaxation attenuates the rapid oscillation in the vicinity of the resonance and thereby reduces the range of frequency where the singular oscillation due to three-photon resonance is effective, and results in narrowing of the resonance structure. Another point of difficulty is that the observed centre frequency of resonance is some tens of kilohertz away from the previously known hyperfine frequencies, and it also varies by a few kilohertz between different experimental runs.

The three-level three-field model seems to offer at least partial explanations for the observed peculiar resonance structure. The model also seems intuitively reasonable in that there is a singularity of some sort when three transitions form a closed loop resonance. As with a set of three coupled mechanical oscillators, the three driving fields need to have exact frequency and phase match in order to sustain the oscillation. On the other hand, the model assumes two simultaneous CW monochromatic fields, whereas in a real dye laser the instantaneous spectrum of the laser may be more likely single mode with occasional mode hop. Therefore,

we may modify the model by allowing only a single optical field with fluctuating frequency. But if the fluctuation is faster than the optical phase relaxation time, then an optical transition will retain the laser phase memory, while the laser jumps back and forth between different frequencies. A simple numerical calculation with two non-overlapping laser pulses each resonant with one of the two optical transitions shows that the singular oscillatory behaviour persists as long as the delay between the two pulses is not longer than the optical phase relaxation time. In this regard, one may note that among the three samples that we have studied, Pr^{3+} in $YAlO_3$ ($T_2 = 35\,\mu s$), Y_2SiO_5 ($110\,\mu s$), and LaF_3 ($6\,\mu s$), we have not observed the resonance structure in LaF_3. Also note that quite often the laser fluctuation can be approximated as a contribution to the optical phase relaxation. A systematic development of the revised model with fluctuating field needs to be carried out.

In summary, we have observed a peculiar resonance structure in an RF-optical double resonance experiment of rare-earth-doped crystals, characterized by a double peak structure of only a few kilohertz width. A numerical study based on a model consisting of three-level atoms interacting with three simultaneous electromagnetic fields shows some of the main features consistent with the experimental data, such as the peculiar resonance lineshape and its dependence on the RF and optical Rabi frequencies.

Acknowledgments

This work is supported by the National Science Foundation (grant ECS 9421304) and the US Air Force Office of Scientific Research (grant F49620-96-1-0395).

References

[1] Harris, S. E., Yin, G. Y., Kasapi, A., Jain, M, and Luo, Z. F., 1996, Electromagnetically induced transparency. In *Coherence and Quantum Optics VII*, edited by J. H. Eberly, L. Mandel and E. Wold (Plenum), pp. 295–304.
[2] Boller, K. J., Imamoglu, A., and Harris, S. E., 1991, *Phys. Rev. Lett.*, **66,** 2593–2596.
[3] Harris, S. E., Field, J. E., and Imamoglu, A., 1990, *Phys. Rev. Lett.*, **64,** 1107–1110.
[4] Zhang, G. Z., Hakuta, K., and Stoicheff, B. P., 1993, *Phys. Rev. Lett.*, **71,** 3099–3102.
[5] Li, Y., and Xiao, M., 1996, *Opt. Lett.*, **21,** 1064–1066.
[6] Ham, B. S., Shahriar, M. S., and Hemmer, P. R., 1997, *Opt. Lett.*, **22,** 1138–1140.
[7] Ham, B. S., Shahriar, M. S., and Hemmer, P. R., 1998, *J. Opt. Soc. Am. B*, **15,** 1541–1544.
[8] Scully, M. O., Zhu, S. Y., and Gavrielides, A., 1989, *Phys. Rev. Lett.*, **62,** 2813–2816.
[9] Harris, S. E., 1989, *Phys. Rev. Lett.*, **62,** 1033–1036.
[10] Alzetta, G., Gozzini, A., Moi, L., and Orriols, G., 1976, *Nuovo Cimento*, **36,** 5–20.
[11] Gray, H. R., Whitely, R. M., and Stroud, C. R., Jr., 1978, *Opt. Lett.*, **3,** 218–220.
[12] Hemmer, P. R, Cheng, K. Z., Kierstead, J., Shahriar, M. S., and Kim, M. K., 1994, *Opt. Lett.*, **19,** 296–298.
[13] Ham, B. S., Hemmer, P. R., and Shahriar, M. S., 1997, *Opt. Commun.*, **144,** 227–230.
[14] Brewer, R. G., and Hahn, E. L., 1975, *Phys. Rev. A*, **11,** 1641–1649.
[15] Shahriar, M. S., and Hemmer, P. R., 1990, *Phys. Rev. Lett.*, **65,** 1865–1868.
[16] Zhao, Y., Wu, C., Ham, B.-S., Kim, M. K., and Awad, E., 1997, *Phys. Rev. Lett.*, **79,** 641–644.

[17] Buckle, S. J., Barnett, S. M., Knight, P. L., Lauder, M. A., and Pegg, D. T., 1986, *Optica Acta*, **33,** 1129–1140.
[18] Lim, M. J., Stievater, T. H., Bucksbausm, P. H., and Conti, R. S., 1999, *Bull. Am. Phys. Soc.*, **44,** 584 (APS Centennial Meeting, Atlanta, GA, Mar. 1999).
[19] Feld, M. S., and Javan, A., 1969, *Phys. Rev.*, **177,** 540–562.
[20] Macfarlane, R. M., and Shelby, R. M., 1981, *Opt. Lett.*, **6,** 96–98.
[21] Salour, M. M., and Cohen-Tannoudji, C., 1977, *Phys. Rev. Lett.*, **38,** 757–760.
[22] Thomas, J. E., Hemmer, P. R., Ezekiel, S., Leiby, C. C., Picard, R. H., and Willis, C. R., 1982, *Phys. Rev. Lett*, **48,** 867–870.
[23] Shelby, R. M., Macfarlane, R. M., and Shoemaker, R. L., 1982, *Phys. Rev. B*, **25,** 6578–6583.
[24] Shelby, R. M., Yannoni, C. S., and Macfarlane, R. M., 1978, *Phys. Rev. Lett.*, **41,** 1739–1742.
[25] Erickson, L. E., 1979, *Phys. Rev. B*, **19,** 4412–4420.
[26] Macfarlane, R. M., Shelby, R. M., and Shoemaker, R. L., 1979, *Phys. Rev. Lett.*, **43,** 1726–1729.
[27] Mitsunaga, M., Yano, R., and Uesugi, N., 1992, *Phys. Rev. B,* **45,** 12760–12768.
[28] Mitsunaga, M., 1993, *Opt. Lett.*, **18,** 1256–1258.
[29] Holliday, K., Croci, M., Vauthey, E., and Wilde, U. P., 1993, *Phys. Rev. B*, **47,** 14741–14752.
[30] Equall, R. W., Cone, R. L., and Macfarlane, R. M., 1995, *Phys. Rev. B*, **52,** 3963–3969.
[31] Hemmer, P. R., Shahriar, M. S., Natoli, V. D., and Ezekiel, S., 1989, *J. Opt. Soc. Am. B*, **6,** 1519–1528.
[32] Sonajalg, H., and Kim, M. K., 1998, *J. Opt. Soc. Am. B*, **15,** 1780–1791.